

## **SUPERCONDUCTOR AND CABLE R&D FOR HIGH FIELD ACCELERATOR MAGNETS AT FERMLAB**

*Invited paper at the International Workshop on  
Progress of Nb-based Superconductors, Feb. 2-3, 2004*

E. Barzi

**Abstract.** This paper presents the results of the strand and cable R&D being performed at Fermilab. Nb<sub>3</sub>Sn strands of various designs and diameters produced with the traditional Internal Tin, Modified Jelly Roll, Restacked Rod Process, and Powder-in-Tube methods were studied. Since superconducting strands in accelerator magnets are used in the form of Rutherford cables, the effect of cabling degradation was measured on extracted strands for a variety of cable geometries and Nb<sub>3</sub>Sn technologies. Critical current sensitivity of impregnated cables to transverse pressure was also measured using a special probe.

### **1. Introduction**

A new generation of superconducting (SC) accelerator magnets with nominal fields of 10-15 T and large operation margins is being developed at Fermilab and elsewhere for future hadron colliders and for upgrading existing machines [1, 2]. This generation is based on the SC intermetallic compound Nb<sub>3</sub>Sn, thanks to its high critical current density,  $J_c$ , critical temperature,  $T_{c0}$ , and upper critical field,  $B_{c20}$ , to the commercial availability of composite Nb<sub>3</sub>Sn strands, and to its affordable cost. In order to reach the required nominal field range with cost effective designs, the Nb<sub>3</sub>Sn strands should meet strong requirements [3] for the level of  $J_c$  at high fields, the effective filament diameter,  $d_{eff}$ , and the value of residual resistivity ratio of the Cu stabilizer. At this time, the most promising technologies for Nb<sub>3</sub>Sn strands produced for SC accelerator magnets appear to be Internal Tin (IT), Modified Jelly Roll (MJR), Restacked Rod Process (RRP) and Powder-in-Tube (PIT). All of them show progress towards the above requirements. Strands with diameters of 0.3-1.0 mm produced using these methods were purchased and studied. Cables of 28 to 60 strands of various diameters and structures (single strands or assemblies of sub-strands), with aspect ratios from 7 to 17, packing factors from 85 to 95%, with and without a stainless steel core were developed and studied. This paper summarizes the results of such R&D effort at Fermilab.

## 2. Critical Current

### A. Intrinsic factors

The critical current,  $J_c$ , of  $Nb_3Sn$  strands is controlled by a few parameters, such as the volumetric fraction of  $Nb_3Sn$  that can be packed in the non-Cu part of a strand and the flux pinning mechanism. The former is affected by strand design parameters such as the Nb filament size, the number of strand sub-elements, and the amount of Sn and of Nb in the non-Cu section. To better understand the effect of filament size during layer growth, a 575°C reaction cycle that provided only partial reaction of the Nb was applied on the same strand drawn down to different diameters [4]. The reacted  $Nb_3Sn$  layer thickness was the same for all strand sizes. It was found that during layer growth, the  $J_c$  dependence on filament size at 12T had an exponential behavior for all tested strand designs. However, after completion of the reaction at 700°C, the  $J_c$  dropped for a filament size below about 1  $\mu m$ .

A larger number of subelements in the strand appeared to increase heat treatment efficiency in forming the  $Nb_3Sn$  A15 phase. This could be inferred by the different times needed for 19 sub-element designs with respect to 37 or 61 subelement designs to reach the peak  $J_c$ . Whereas the former required 50 to 70 h, the latter needed only 40 to 50 h [4].

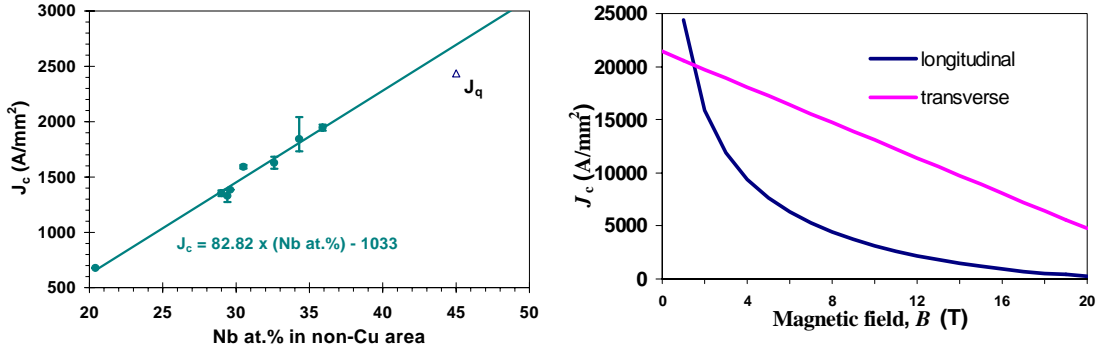


Fig. 1. Left:  $J_c$  (12 T, 4.2 K) as a function of the atomic percentage of Nb in the non-Cu section. The triangle data point represents a quench current density. Right:  $J_c$  (12 T, 4.2 K) of  $Nb_3Sn$  vs. magnetic field as predicted by [6] for both ‘transverse’ and ‘longitudinal’ pinning.

The  $J_c$  of IT strands is proportional to the atomic percentage of Nb in the non-Cu area of a wire. This is shown in Fig. 1 (left), where the  $J_c$ ’s at 12 T and 4.2 K were produced by different strands having undergone similar heat treatment cycles. To reach a  $J_c$ (12T, 4.2K) of 3000 A/mm² requires about 50at.% Nb with the present IT technology. To judge whether  $Nb_3Sn$  can be improved beyond this restriction, the flux pinning mechanisms need further understanding.

Progress towards understanding the flux pinning mechanisms in  $Nb_3Sn$  was made with a model for  $J_c$  in granular A15 superconductors [5]. It is generally agreed that NbTi and  $Nb_3Sn$  show very different scaling behavior with respect to magnetic flux density. Many authors have attributed this difference to different mechanisms for flux motion: the scaling behavior of NbTi has been associated with pin breaking, while that of  $Nb_3Sn$  has been identified with flux shearing. In [6],  $J_c$  is determined solely by grain boundary pinning. However, this single mechanism can lead to two different scaling laws because of the anisotropy of the pinning forces. This model predicts that the  $J_c$ (12T, 4.2K) of  $Nb_3Sn$  could be improved by a factor of 4 to 5, as shown in Fig. 1 (right), by finding a way to increase the transverse flux pinning

contribution (typical of NbTi) with respect to the longitudinal one that prevails in current Nb<sub>3</sub>Sn materials.

#### B. Heat Treatment (HT)

The reaction cycle is a critical step in the manufacturing process of a magnet. During HT several metallurgical phases are created and eliminated in the course of the Sn diffusion through the Cu matrix and of the Nb<sub>3</sub>Sn formation processes. The SC and mechanical properties of the superconductor are obtained during this operation. Some examples of HT cycles are shown in Fig. 2, where the duration of the nominal company cycles was reduced by 2 to 4 times by increasing the last step temperature. The low temperature steps of the HT are programmed to diffuse the Sn into the Cu, but also to prevent leakage of Sn rich liquid phases, which has become a concern for high  $J_c$  Nb<sub>3</sub>Sn strands [6]. The high temperature steps of the HT are planned to form the adequate Nb<sub>3</sub>Sn phase volume, with a stoichiometric A15 layer composition and optimum microstructure. Additional factors to be included in HT optimization are preferably short durations and high strand RRR. The RRR, defined as the ratio of the Cu resistivity at room temperature over its residual resistivity, is a means to measure strand Cu purity, which is important for strand stabilization and magnet quench protection. Typical values for the present technologies are of about 200 for PIT and IT. For MJR, the RRR depends strongly on the Nb barrier thickness, ranging from 5 to 160 for barrier thicknesses of 3 to 6  $\mu\text{m}$  [7]. A low RRR indicates damage of the internal structure of the strand and Sn leakage into the surrounding Cu stabilizer. The RRR was found to depend also on the heat treatment cycle and, in some instances, to be affected by cabling [8]. All Nb<sub>3</sub>Sn technologies, and especially the PIT, display a large fraction of voids after reaction. Reducing these voids may reduce  $J_c$  strain sensitivity [9].

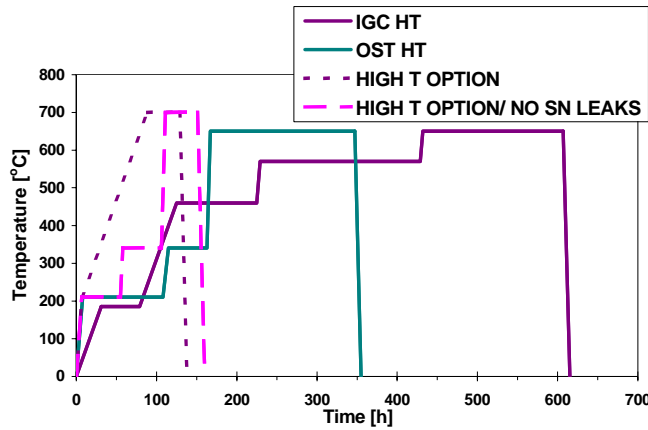


Fig. 2. Examples of Nb<sub>3</sub>Sn HT cycles.

In order to knowledgeably plan the low temperature steps of the HT, the growth kinetics of Cu-Sn intermetallics was investigated as a function of duration and temperature [10]. The diffusion constants of  $\eta$ ,  $\epsilon$  and  $\delta$  phases between 150°C and 550°C (*i.e.* within the temperature ranges of solid diffusion) were evaluated as fitting parameters by minimizing the  $\chi^2$  function of the layer thickness measurements versus HT time and temperature using the parabolic growth law. This is shown in Fig. 3 for the  $\epsilon$  phase between 227°C and 415°C. In order to provide “infinite” sources of Cu and Sn, Cu-Sn sample models were realized by

casting liquid Sn into Cu containers, and heat treating them in pyrex tubes with nitrogen coverage. For an accurate data analysis, statistical and systematic errors were determined. Next the behavior of IT and MJR Nb<sub>3</sub>Sn composites was compared with the model predictions to check the impact of both radial geometry and Sn depletion. The results in the strands show that before depletion of the Sn, the average thickness of the Cu-Sn phase is consistent with that formed in the Cu-Sn models. A way to prevent leaks of Sn rich phases, characterized by low melting points, is to convert them into higher melting phases. Other results of the study on strands show that despite a complete transformation of pure Sn into a higher temperature melting phase takes excessively long times at temperatures below the melting point of the Sn, crossing the Sn melting point without a preliminary HT step is sufficient to create Sn leakages in cables. Also, in typical strands, the Sn cannot be uniformly distributed around all the Nb filaments prior to the beginning of the A15 phase formation, since the inner ring of the filaments is immersed into  $\epsilon$  phase, while the outer ring is immersed in  $\alpha$  phase and/or pure Cu. However, it is not yet clear to what extent matrix heterogeneity influences Nb-Sn diffusion.

The layer growth and SC properties of Nb<sub>3</sub>Sn were also investigated as a function of the heat treatment duration and temperature for an IT and a PIT strand at 650°C, 700°C and 750°C [11]. For all times and temperatures, the Nb<sub>3</sub>Sn layer thickness, the critical current at 4.2 K as a function of magnetic field, and the RRR were measured. The upper critical field was obtained through parameterization. Results are shown in Fig. 4 for the PIT strands. Using these results, an optimum Nb filament size was determined with respect to the SC properties.

The feasibility of winding partly reacted cables to reduce the magnet manufacturing time was also explored. Some MJR and ITER Nb<sub>3</sub>Sn strands have been partially reacted to convert the Sn to the  $\eta$  and  $\epsilon$  phases, thus suppressing the risk associated with the liquid phases of Sn, and then plastically strained to figure out the amount of cabling and/or winding degradation. After completion of the reaction cycle at 700°C, the  $I_c$  was measured and compared with that obtained with an uninterrupted cycle. No  $I_c$  degradation was observed with preliminary heat treatments at 210°C and 400°C [12].

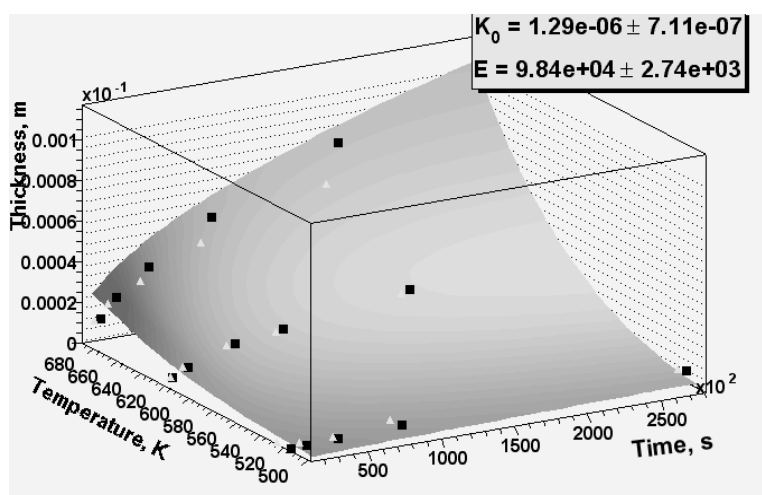


Fig. 3. Measured (black squares) and expected (white triangles) thickness of the  $\epsilon$  Cu-Sn intermetallic phase between 227°C and 415°C versus HT parameters. The diffusion frequency,  $K_0$ , is shown in [cm<sup>2</sup>/s], and the activation energy,  $E$ , in [J/mol].

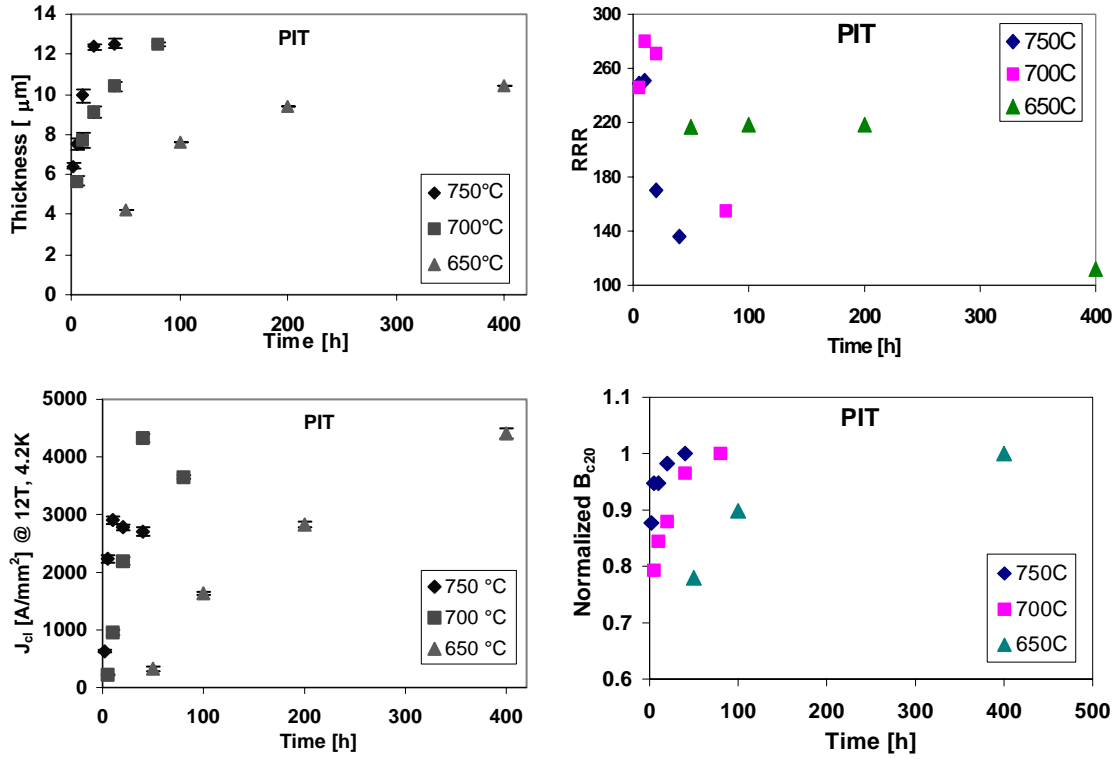


Fig. 4. Top left:  $\text{Nb}_3\text{Sn}$  layer growth; Top right: RRR; Bottom left: layer critical current density  $J_c$  at 12 T and 4.2 K; and Bottom right: normalized  $B_{c20}$ , for a PIT strand as a function of HT duration at 750°C, 700°C and 650°C.

### C. Extrinsic factors

The  $I_c$  of a virgin strand can be substantially degraded during cabling, magnet fabrication and operation. That is why studies of strand plastic deformation during cabling and transverse pressure on the strand in cable were performed.

Short samples of 28-strand Rutherford cable with packing factors (PF) in the 85 to 95% range were fabricated by varying the cable thickness. The results of  $I_c$  measurements made on round virgin strands were compared with those made on strands extracted from cables [13]. The  $I_c$  degradation at 4.2 K and 12 T, expressed as the  $I_c$  of an extracted strand normalized to the  $I_c$  of the virgin strand, is shown in Fig. 5 (left) as a function of  $PF$ . This plot also shows a comparison with results obtained from previous studies [8, 14], which entailed cables fabricated with different cabling machines. One can observe good consistency among cables made with similar strands. In the  $PF$  range of 88-90%, the  $I_c$  cabling degradation at 12 T was 7 to 9% practically for all tested strands. There is no observable difference between rectangular and keystone cables having the same  $PF$ .

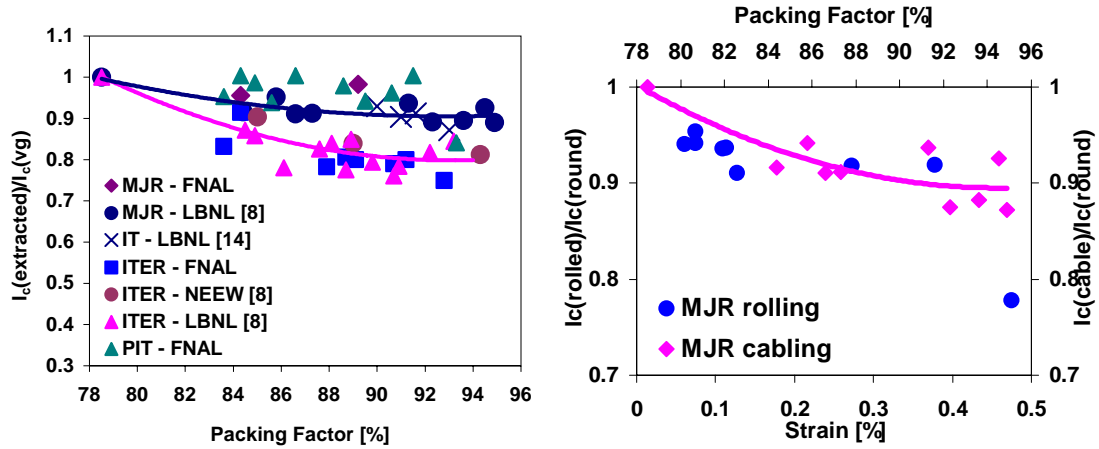


Fig. 5. Left: Normalized  $I_c$  at 4.2 K and 12 T as a function of packing factor for the extracted IT, MJR and PIT  $\text{Nb}_3\text{Sn}$  strands. Right: Effect on the  $I_c$  of rolling versus cabling for the MJR strand at 4.2 K and 12 T.

In order to simulate plastic deformation during the cabling process,  $\text{Nb}_3\text{Sn}$  strands of different technologies were rolled down to various sizes, heat treated and tested [13]. Strand deformation was characterized by strain, defined by  $(d-t)/d$ , where  $d$  is the original round strand diameter and  $t$  the strand thickness after rolling. The critical current of the rolled strands was then compared with that of the same strand extracted from cables with various packing factors. Some results are shown in Fig. 5 (right) for the MJR. By matching at best the data points for the rolled and extracted strands, one can find a range of strain for rolled strands where a reasonably good correlation of  $I_c$  degradation is observed between the latter and extracted strands. Therefore, it appears that rolling down strands is an excellent method to simulate the effect of  $I_c$  degradation due to cabling, and can therefore be used instead of it.

The studies of the sensitivity of  $\text{Nb}_3\text{Sn}$  strands within a reacted and impregnated Rutherford cable to transverse pressure were performed using a special fixture [15, 16]. To prevent current sharing, the housing cable is made of Cu. A summary of the results for a number of  $28 \times 1$  mm cables are shown in Fig. 6. It appears that in the case of the ITER material,  $I_c$  degradation at 12 T is negligible and reversible up to about 140 MPa of pressure. Irreversibility begins at pressures somewhat larger than this value, with a 5% residual degradation at about 150 MPa. An ampler statistics is needed to confirm and better quantify the irreversibility onset. However, at about 200 MPa of pressure, samples show an  $I_c$  degradation of 70 to 80% at 12 T, most of which is maintained all along the unloading cycle down to 27.8 MPa. In the case of the MJR strands, the onset pressure of irreversibility was found also to be at around 140 MPa. After loading up to about 210 MPa, where  $I_c$  degradation was on the order of 20%, the residual degradation at 27.8 MPa was about 30%. For the PIT, up to about 60 MPa of pressure the  $I_c$  degradation was found to be reversible for at least one sample, and smaller than 15% for all samples. The onset of irreversibility should therefore occur beyond 60 MPa. However, at 100 MPa the  $I_c$  degradation was already around 20% for all samples, and appeared to rapidly decrease at larger loads. After loading up to about 200 MPa, the  $I_c$  degradation was on the order of 90%, all of it permanent.

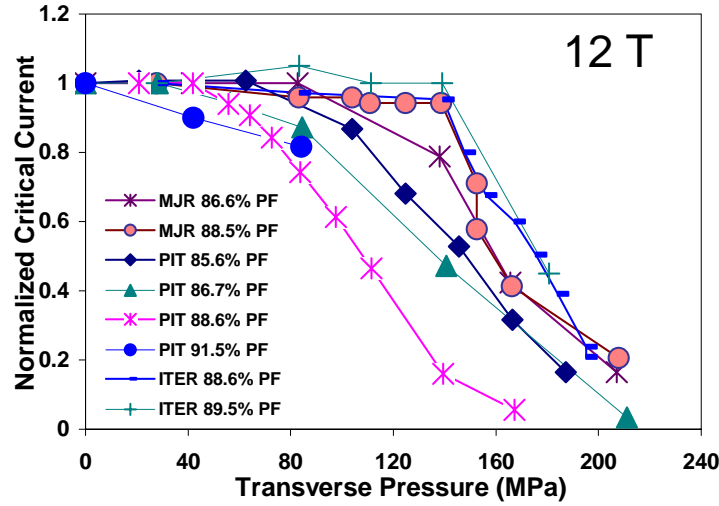


Fig. 6. Normalized  $I_c$  vs. transverse pressure for all samples tested at 12 T.

## 2. Magnetization and Stability

A low level of strand magnetization is important for achieving good field uniformity and stability in accelerator magnets. Due to technological constraints, all high  $J_c$   $Nb_3Sn$  strands have a large  $d_{eff}$ , which is responsible for magnetization. For 1 mm high  $J_c$  strands, the  $d_{eff}$  ranges from about 50  $\mu m$  for PIT to 110  $\mu m$  for MJR [17], and to even larger values for IT [7]. The  $d_{eff}$  is calculated directly from magnetization loops performed between 10 and 13 T with a balanced coil magnetometer [18], by measuring  $\mu_0 \Delta M$  and  $I_c$  at 12 T. Large  $d_{eff}$  and high  $J_c$  result in large hysteretic magnetization and AC losses and, what is even more important, lead to magnetic instabilities in  $Nb_3Sn$  strands. Magnetic instabilities (flux jumps) are assessed by magnetization loops between 0 and 3 T as in Fig. 7 (left). Magnetic instabilities limit also the strand current carrying capability causing premature quenches at low field as shown in Fig. 7 (right). It was found that flux jumps for a same strand depend also on the reaction cycle [17]. The effect of large flux jumps in  $Nb_3Sn$  strands on magnet quench performance was observed experimentally during the  $Nb_3Sn$  model tests [19, 20].

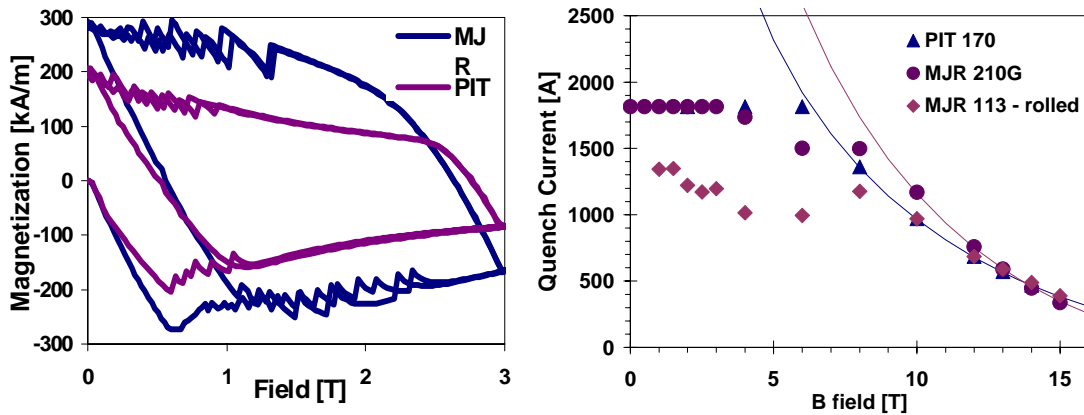


Fig. 7. Left: Magnetization curves per strand volume for a 1 mm MJR and a 1 mm PIT strand. Right: Critical current instabilities observed at low fields during transport measurements.

### 3. Nb<sub>3</sub>Sn Anisotropic Expansion

It is known that Nb/Sn composite strands expand after reaction due to formation of the Nb<sub>3</sub>Sn phase. In round strands this expansion is isotropic. However, an anisotropic volume expansion was observed in some Nb<sub>3</sub>Sn models. While the cable width did not change significantly, the thickness increased by more than expected. To check the hypothesis that the plastic deformation impressed during cabling would release itself during HT, Nb<sub>3</sub>Sn strands of different technologies were rolled down to various sizes. The resulting thickness and width of the deformed strands were measured before and after heat treatment and compared with cable measurements. The thickness expansion was always larger than the width expansion for both strands and cables. Furthermore, the amount of volume expansion appeared to depend on the strand technology and to be a function of the Nb-Sn content [21].

### 4. Conclusions

SC strands and cables determine magnet performance and cost, and are the key component of high field accelerator magnets. Several designs of Nb<sub>3</sub>Sn strands of different diameters produced using the IT, MJR, RRP and PIT methods were studied. Study and optimization of HT has allowed a reduction of reaction times by a factor of 2 to 4 preserving the highest possible superconducting phase volume and an optimal microstructure. An additional option to reduce HT duration during magnet manufacturing is to partially react strands or cables before utilization. It was found that this could be done without any substantial I<sub>c</sub> degradation. The impact of the strand design on the I<sub>c</sub> was also better understood and quantified. A model developed for A15 conductors suggests that the intrinsic high field J<sub>c</sub> of Nb<sub>3</sub>Sn could be improved by a factor of 4 to 5. Rutherford-type cables of various designs made of different Nb<sub>3</sub>Sn strands were developed and studied. The effects of plastic deformation during cabling and of strand compression in the cable on the strand I<sub>c</sub> degradation were measured for all the above Nb<sub>3</sub>Sn technologies. All these studies are very important for the progress in the R&D to produce accelerator magnets with fields in the 10 T to 15 T range, and will lead to reaching this goal in a few years from now.

### References

- [1] "Design Study for a Staged Very Large Hadron Collider", Fermilab-TM-2149, June 4, 2001.
- [2] T. M. Taylor, "Superconducting Magnets for a Super LHC", EPAC 2002, Paris, June 3-7, 2002, p. 129.
- [3] G. Ambrosio et al., "Superconductor Requirements for the HFM Program at Fermilab", FNAL TD-99-073, Dec. 15, 1999.
- [4] E. Barzi et al., "Heat Treatment Optimization of Internal Tin Nb<sub>3</sub>Sn", IEEE Trans. App. Sup., v. 11, No. 1, March 2001, p. 3573.
- [5] J. McDonald et al., "A Model for J<sub>c</sub> in Granular A-15 Superconductors", IEEE Trans. Appl. Sup., v. 11, No. 1, 2001, p. 3884.
- [6] E. Barzi et al., "Progress Report on Superconducting Strand and Cable R&D", FNAL TD-01-013, Feb. 14, 2001.
- [7] E. Barzi et al., "Study of Nb<sub>3</sub>Sn Strands and Cables for Fermilab's Common Coil Dipole Models", Advances in Cryogenic Engineering, v. 48A, p. 933, 2002.
- [8] E. Barzi et al., "Strand Critical Current Degradation in Nb<sub>3</sub>Sn Rutherford Cables", IEEE Trans. Appl. Sup., v.11, No. 1, March 2001, p. 2134.
- [9] D. R. Dietderich et al., "Critical Current of Superconducting Rutherford Cable in High Magnetic Fields with Transverse Pressure", IEEE Trans. Appl. Sup., V. 9, 1999, p. 122.

- [10] S. Mattafirri et al., "Kinetics of Phase Growth in the Cu-Sn System and Application to Composite Nb<sub>3</sub>Sn Strands", IEEE Transactions on Applied Superconductivity, V. 13, No. 2, June 2003, p. 3418.
- [11] E. Barzi et al., "Nb<sub>3</sub>Sn Phase Growth and Superconducting Properties During Heat Treatment", IEEE Transactions on Applied Superconductivity, V. 13, No. 2, June 2003, p. 3414
- [12] J.-M. Rey et al., "Effect of Partially Reacting Nb<sub>3</sub>Sn before Magnet Winding on the Strand Critical Current", Advances in Cryogenic Engineering, V. 48A, p. 1001, 2002.
- [13] E. Barzi et al., "Development and Study of Rutherford-type Cables for High-field Accelerators Magnets at Fermilab", Superconductor Science and Technology, special issue, v. 17, issue 5, p. 213.
- [14] E. Barzi et al., "Study of Strand Critical Current Degradation in a Rutherford Type Nb<sub>3</sub>Sn Cable", Advances in Cryogenic Engineering, v. 46B, p. 1091, 2000.
- [15] E. Barzi et al., "A Device to Test Critical Current Sensitivity of Nb<sub>3</sub>Sn Cables to Pressure", Advances in Cryogenic Engineering, V. 48A, p. 45, 2002.
- [16] E. Barzi et al., "Sensitivity of Nb<sub>3</sub>Sn Rutherford-type Cables to Transverse Pressure", E. Barzi, T. Wokas, A. V. Zlobin. EUCAS 2003, Sorrento (Naples), Italy, Sept. 14-18, 2003.
- [17] E. Barzi et al., "Study of Nb<sub>3</sub>Sn Strands for Fermilab's High Field Dipole Models", IEEE Trans. Appl. Sup., v. 11, No. 1, March 2001, p. 3595.
- [18] C. Boffo, "Magnetization Measurements at 4.2 K of Multifilamentary Superconducting Strands", FNAL TD-99-074, 1999.
- [19] G. Ambrosio et al., "Development and Test of a Nb<sub>3</sub>Sn Racetrack Magnet using React and Wind Technology", Advances in Cryogenic Engineering, V. 47A, p. 329, 2002.
- [20] S. Feher et al., "Test Results of Shell-type Nb<sub>3</sub>Sn Dipole Coils", MT-18, Japan, October 2003.
- [21] N. Andreev et al., "Volume Expansion of Nb<sub>3</sub>Sn Strands and Cables during Heat Treatment", Advances in Cryogenic Engineering, V. 48A, p. 941, 2002.